Transient Adsorption Studies of Automotive Hydrocarbon Traps

Jing Luo
Ford Research and Advanced Engineering, Dearborn, MI 48121

Chemical and Biomolecular Engineering, University of Pennsylvania, Philadelphia, PA 19104

Robert W. McCabe and Mark A. Dearth
Ford Research and Advanced Engineering, Dearborn, MI 48121

Raymond J. Gorte
Chemical and Biomolecular Engineering, University of Pennsylvania, Philadelphia, PA 19104

DOI 10.1002/aic.14477
Published online April 25, 2014 in Wiley Online Library (wileyonlinelibrary.com)

A chromatographic adsorption unit was designed and built to study the adsorption of alkanes in zeolites for the hydrocarbon trap systems in three-way catalysts, to assist in the selection of optimal materials for this application. The experimental apparatus used a zeolite bed in place of the column in an ordinary gas chromatograph and could be accurately modeled to determine the adsorption equilibrium constants for simple alkanes in MFI zeolites. The adsorption of iso-pentane was studied in BEA zeolites with varying Si/Al_2 ratios, before and after ex situ zeolite aging simulating engine exhaust, and in the presence of water vapor. The elution times were shown to depend directly on the zeolite adsorption capacity. The primary effect of water was to decrease the iso-pentane adsorption capacity by partial filling of the zeolite pores through adsorption of water at acid sites. Some implications of this work for choosing the best materials for hydrocarbon trapping are discussed. © 2014 American Institute of Chemical Engineers *AIChE J*, 60: 2875–2881, 2014
Keywords: chromatographic adsorption, automotive hydrocarbon trap, zeolite, alkane adsorption, heat of adsorption

Introduction

Catalyzed hydrocarbon trap systems (HCTs) offer a potential technological solution for capturing and converting emissions of hydrocarbon and organic species that break through the main, close-coupled (CC), three-way catalytic converters (TWCs) during cold-start and warm-up of gasoline and flex-fuel vehicles. Previous studies have been split between laboratory investigations of various adsorber materials[1–18] and applied studies demonstrating HCT performance at the vehicle level—the latter documented almost exclusively in the Society of Automotive Engineers literature.[19–25] To date, commercial introduction of HCT technology has been limited due to cost, complexity, durability issues, and low overall storage and conversion efficiencies. Moreover, advances in both cold-start combustion technology and rapid TWC heat-up strategies have allowed conventional TWC technology to keep pace with more stringent emission standards and useful life requirements.[26] The latter situation may change over the next 10 years, however, as the entire vehicle fleet moves to low-emission vehicle mandates such as LEV-III, especially for flexible-fuel vehicles certified on both gasoline and E85 fuels.[27] In addition, broader application of turbochargers presents a new challenge to the catalytic converter system owing to the delay they impose on catalyst warm-up. For these reasons, automakers and catalyst suppliers continue to investigate the potential of HCT technologies.[28]

The simplest embodiment of an HCT is the so-called passive approach in which an underbody (UB) TWC (in a combined CC + UB system) is replaced with a catalyzed HCT. The catalyzed HCT differs from a conventional TWC only in that the monolith washcoat consists of an underlayer of zeolite material and a topcoat of TWC material (rather than the common practice of two coats of TWC material of differing composition). Ideally, hydrocarbons that break through the CC-TWC during the first 30 s or so adsorb on the zeolite material and then desorb and combust over the top layer of TWC material as the trap warms up. In practice, a substantial fraction of the HC species desorbs before the catalyst is hot enough to combust them. This situation is exacerbated by the large amount of water that condenses along with the HC at the front of the trap and then gradually revaporizes and elutes through the remainder of the trap as the thermal front traverses the system. To this end, the HCT system resembles a temperature-programmed chromatographic adsorber in which the various HC species and water are injected into the trap as a diffuse 30 s pulse and then elute at rates governed by the concentrations and differential heats of adsorption of each species.

Because the HC traps require a complex set of processes, including adsorption (in the presence of water), desorption, transport, and reaction, the choice of materials that would be most effective for this application remains unclear. For example, it is not known whether the presence of acid sites

Correspondence concerning this article should be addressed to R. J. Gorte at gorte@seas.upenn.edu.

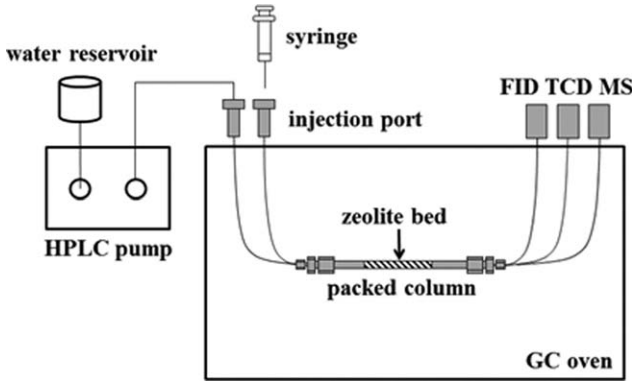

Figure 1. Schematic of the experimental apparatus for HC trapping measurement.

is beneficial or harmful; the effects of hydrothermal aging on the trapping properties of the zeolite adsorbents are also unclear. Therefore, this study was initiated to break down the complicated HC trapping processes into fundamental steps and aid in the design of trapping materials. To this end, we report the design and construction of a simple laboratory gas chromatographic adsorber and demonstrate its effectiveness for determining elution times and corresponding differential heats of adsorption, both in the absence and presence of water. We have focused on light alkanes, at concentrations similar to what will be found in actual applications, because these are likely to be the most difficult components to trap and react.

Experimental

A schematic of the experimental apparatus used in making the HC-trapping measurements is shown in Figure 1. The equipment consisted of a gas chromatograph (6890 Series, Agilent/HP) with the normal GC column replaced by a $\frac{1}{8}$ inch-stainless steel tube (12-cm long, 2.1-mm ID) packed with zeolite material retained by glass wool plugs. Most measurements used 0.08 g of zeolite, which gave a bed length of approximately 4 cm. The inlet to the sample column consisted of two injection ports made from 0.35-mm ID, silica capillary tubes. One of the injection ports allowed introduction of gaseous hydrocarbons using a gas-tight syringe, while the other was connected to a HPLC pump (Series 1050, HP) to allow liquid water to be added continuously. The injection port used for adding water was heated to approximately 330 K and filled with glass wool to enhance vaporization. Separate streams of He (UHP grade, Airgas) were admitted into the two injection ports before merging at the inlet of the packed column. In all experiments, the total flow rate of carrier gas into the column was fixed at 25 mL/min and the residence time for nonadsorbing gases was approximately 2 s. Broadening of effluent peaks in the absence of adsorption was also of order 2 s The effluent concentrations from the column could be monitored using either a thermal conductivity detector, a flame ionization detector, or a mass selective detector. The gases used to introduce the alkanes into the column were all obtained from Airgas and had the following compositions: propane (1000 ppm balanced in N_2), iso-pentane (5% balanced in N_2), *n*-hexane (5% balanced in N_2), and *n*-octane (1000 ppm balanced in N_2).

The zeolite samples used in this study are listed in Table 1 together with some of their physical characteristics. All of the zeolite powders were calcined in flowing 5% oxygen at 773 K for 1 h to place them in the protonic form and to remove any residual organic materials. Aged samples were generated by placing the fresh zeolite powder in a quartz boat in a tube furnace and subjecting the samples to a 4-mode aging cycle (in 10% H_2O) at a total flow rate of 6.4 L/min and gas temperature of 750°C. The 4-mode cycle is a simplified laboratory adaptation of Ford's 4-mode dynamometer aging protocol and consists of: (1) 41 min "stoich" (i.e., neutral) (N_2), (2) 6 min rich (3%CO/1%H_2/N_2), (3) 5 min neutral (N_2), and (4) 8 min lean (3%O_2/N_2). The cycle was repeated 25 times for a total aging time of 25 h. Prior to incorporating the zeolites into the column for HC-trapping measurements, they were pressed into thin wafers and then sieved so that only particles between 250 and 500 μm were included.

It was determined that the pore volume of the zeolite sample is a critical parameter in these measurements.[29] Although the pore volume of an ideal zeolite is determined by the structure of that zeolite, the capacity of real materials is usually less than the ideal value due to the presence of amorphous material in the sample or to partial pore filling of the structure by nonframework material. In this study, the adsorption capacities for the various BEA samples were determined by measuring their weight changes on exposure to iso-pentane at room temperature. The weight changes were obtained in a flow thermal gravimetric analysis (TGA) system at the Ford Laboratory by simply switching the gas composition from pure N_2 to N_2 with 5% iso-pentane. In Table 1, these adsorption capacities are reported as pore volumes and were calculated assuming the iso-pentane within the pores packed with its liquid density. The values reported in Table 1 are comparable to those reported previously for the BEA structure, 0.22 cm^3/g,[30] and changes in the iso-pentane uptakes provide a good comparison between BEA samples. Iso-pentane is also a representative component of hydrocarbons present in the exhaust stream. It is noteworthy that the aged samples, in particular, have lower pore volumes than the fresh samples, either due to the presence of amorphous material in the samples or from having partially filled pores.

Model Development

The results for the HC-trapping measurements were analyzed by treating the zeolite bed as a tubular reactor with axial dispersion and perfect radial mixing. Diffusion within the zeolite wafers and crystallites was assumed to be rapid. With these conditions, the balance on the gas-phase and adsorbed-phase concentrations, C and n, is given by Eq. 1 [31]

$$D\frac{\partial^2 C}{\partial x^2} - U\frac{\partial C}{\partial x} = \varepsilon\frac{\partial C}{\partial t} + (1-\varepsilon)\rho\frac{\partial n}{\partial t} \tag{1}$$

The usual Danckwerts boundary conditions are given in Eqs. 2 and 3

$$UC - D\partial C/\partial x = UC_0(t) \qquad at \qquad x = 0 \tag{2}$$

$$\partial C/\partial x = 0 \qquad at \qquad x = L \tag{3}$$

The initial concentration in the column is assumed to be zero and the input to the column, $C_o(t)$, is a pulse given by Eq. 4. The length of the pulse, t_o is very short compared to the residence time

Table 1. Physical Characteristics of Zeolite Samples: Si/Al_2 Ratio of BEA38 was Obtained from XRF Analysis by Ford X-Ray Laboratory, While the Others were from Zeolyst Product Analysis; Saturation Gravimetric Uptakes for Iso-Pentane on BEA Samples were Measured by TGA at Ford Laboratory

				Iso-Pentane Uptakes (cm^3/g)[a]	
Zeolite Type	Si/Al_2	Cation Form	Supplier	Fresh Sample	Aged Sample
MFI	280	Ammonium	Zeolyst	–	–
BEA	24	Ammonium	Zeolyst	0.196	0.147
BEA	38	Hydrogen	–	0.229	0.185
BEA	200	Hydrogen	Zeolyst	0.163	0.160

[a]Assumes that the iso-pentane packed at its liquid density into the BEA zeolite.

$$C_o(t)=C_o \quad for\ 0<t<t_o$$
$$C_o(t)=0 \quad for\ t>t_o \tag{4}$$

To relate C and n, we assumed adsorption equilibrium is established at every position and that the isotherm is linear, as shown in Eq. 5

$$n=aKC \tag{5}$$

The various parameters in these equations are listed in the Glossary. With the exception of the product of the equilibrium constant, K, and the effective zeolite fraction, a, all of the parameters in the above equations can be determined with reasonable accuracy from other sources. (The solutions to the above equations will always be in terms of the product of K and a.) For example, the axial dispersion coefficient, D, can be estimated from correlations of the Peclet number (UL/D) as a function of Reynolds number.[31] Values for the fluid velocity (U), the bed porosity (ε), and bed length (L) were all measured. The effective zeolite fraction, a (g/g), accounts for the variable pore volumes of the various zeolite samples and is equal to the measured pore volume divided by the ideal pore volume of that zeolite structure.

In the HC-trapping experiment, the measured value is the gas-phase concentration at the exit from the bed, $C(L,t)$. Therefore, we solved the above equations using Finite Fourier Transforms to obtain the solution given in Eq. 6 for $t>t_o$

$$C(L,t)=\sum_{n=1}^{\infty}\frac{C_0\omega_n(0)\omega_n(1)e^{Pe/2}}{(\lambda_n^2+Pe^2/4)}\left[e^{\frac{D(\lambda_n^2+Pe^2/4)t_o}{[\varepsilon+a(1-\varepsilon)\rho K]L^2}}-1\right]e^{-\frac{D(\lambda_n^2+Pe^2/4)t}{[\varepsilon+a(1-\varepsilon)\rho K]L^2}} \tag{6}$$

Here, λ_n are the eigenvalues calculated from Eq. 7

$$\cot(\lambda_n)=\frac{\lambda_n^2-Pe^2/4}{Pe\lambda_n} \tag{7}$$

and ω_n are the eigenfunctions, Eq. 8

$$\omega_n(x/L)=\frac{Pe\sin(\lambda_n x/L)/2+\lambda_n\cos(\lambda_n x/L)}{\sqrt{(\lambda_n^2+Pe^2/4+Pe)/2}} \tag{8}$$

It is worth noting that the above model assumes diffusion into the sample wafers and into the zeolite crystals is rapid. In both cases, the characteristic time for diffusion is given by the square of the characteristic lengths divided by the appropriate diffusivity. For diffusion into the wafers, the characteristic length (100 μm) and diffusivity (0.1 cm^2/s) yield a characteristic time of 10^{-3} s. For diffusion into the crystallites, the characteristic length (0.5 μm) and diffusivity (1.5×10^{-7} cm^2/s is the value reported for iso-octane in BEA at 298 K)[32] make the characteristic time less than 10^{-2} s. Because these times are very short compared to the elution times in the column, the assumption that diffusion can be neglected is reasonable.

Results

To allow comparison of experiments to the mathematical model, we first established conditions for which the linear isotherm, Eq. 5, was appropriate. Because the linear isotherm will always hold at low adsorbate coverages, we conducted a pulse study with iso-pentane on BEA38 at 393 K as a function of amount of iso-pentane injected in the initial pulse. Figure 2 shows normalized elution profiles as a function of dose size between 2 and 16 μmol. Except for the largest dose, the shape of the profiles was unaffected. Since the typical dose in this study was 2–4 μmol of adsorbate, the linear isotherm is expected to be valid. It is worth noting that a 4 μmol pulse evenly distributed over the entire zeolite bed would give a loading of 0.0036 g iso-pentane/g (0.0058 cm^3/g), which is less than 3% of the saturation uptake determined for this sample, 0.229 cm^3/g. Furthermore, this loading is comparable to those in functioning HC traps, where design targets are set far below saturation levels to avoid slip.

HC-trapping experiments with iso-pentane on BEA38 were then conducted as a function of temperature, with results shown in Figure 3a. Not surprisingly, the peak elution time, t_p, and the spread of the elution curve decreased with increasing temperature. For example, t_p decreased from 1067 s at 373 K to 106 s at 433 K. To check whether diffusion from the gas phase into the sample wafers could be important, we also performed experiments with thinner wafers (180 to 250 μm rather than 250 to 500 μm) and with the He

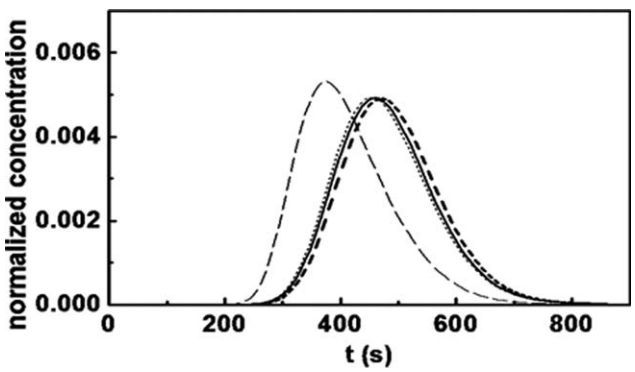

Figure 2. Normalized elution profiles for iso-pentane injection in BEA38 at 393 K, with different dose sizes: dash line (---) 16.7 μmol, dotted line (···) 4.5 μmol, solid line (—) 3.3 μmol, bold dash line (---) 2.2 μmol.

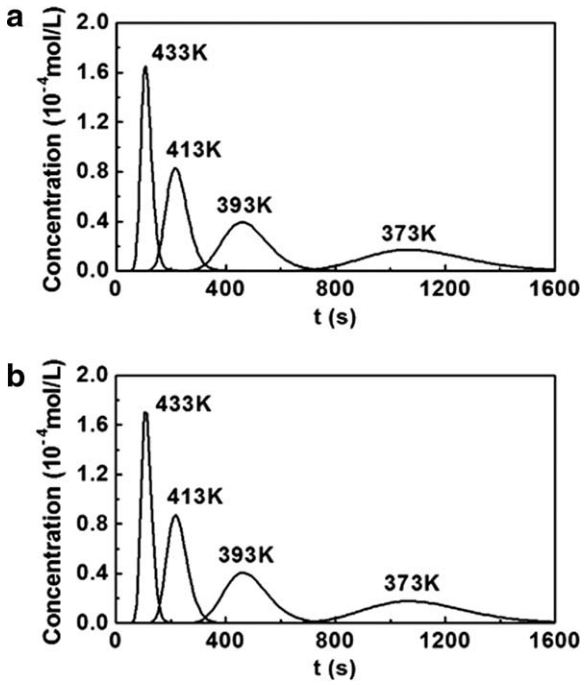

Figure 3. (a) Experimental elution profiles for iso-pentane injection through BEA38 as a function of temperature; (b) elution curves calculated from Eq. 6 by adjusting only the product of *a* and *K*.

Parameters used were as follows:

$C_0 = 6.68\times10^{-3}$ mol/L; $t_0 = 1.2$ s

$L = 0.04$ m; $U = 0.15$ m/s

$\varepsilon = 0.35$ m^3/m^3; $\rho = 1300$ g/L

$D_. = 8.57\times10^{-5}$ m^2/s; $Pe = 70.01$

$a\cdot K_{373K} = 4.942$ L/g; $a\cdot K_{393K} = 2.142$ L/g

$a\cdot K_{413K} = 1.001$ L/g; $a\cdot K_{433K} = 0.497$ L/g.

carrier replaced by N_2. Because the binary gas-phase diffusivity of iso-pentane in N_2 should be significantly smaller than in He, the elution curves would be expected to shift to longer times with N_2 if diffusion were important. However, the results with thinner wafers and with the N_2 carrier were indistinguishable from those observed with thicker wafers and with the He carrier. Although, we were not able to vary the size of the zeolite crystallites and diffusion in the crystallites would not be affected by the carrier-gas composition, the length scale for the crystallites is so much smaller than that for the sample wafers that intracrystalline diffusion is not likely rate limiting, as discussed earlier.

Figure 3b was calculated from Eq. 6 by fitting the elution curves, adjusting only the product of a and K. In this calculation, the inverse of the Pe number and the dispersion coefficient, D, were determined from correlations to be 0.014 and 8.57×10^{-5} m^2/s, respectively, while the sample density and bed porosity were measured. Only K was allowed to vary with temperature. The fit of the model to both the peak elution times and to the shapes of the elution curves is very good as seen by comparing Figures 3a, b.

The good fit between experiment and calculation does not prove that the equilibrium constant extracted from the calculation is accurate. As an additional test of the approach, we performed a similar series of experiments with propane, n-hexane, and n-octane over a range of temperatures in an MFI zeolite. The fit of the calculations to the experiments, using the same Pe number and dispersion coefficient, was again excellent. We then plotted the logarithm of the calculated $a \times K$ values as a function of 1/T, as shown in Figure 4. Using Eq. 9

$$\frac{d\ln K}{d(1/T)} = -\frac{\Delta H}{R} \tag{9}$$

we calculated the heats of adsorption for the three adsorbates to be 40 ± 2 kJ/mol for propane, 68 ± 2 kJ/mol for n-hexane, and 90 ± 2 kJ/mol for n-octane. The values for propane and n-hexane are in excellent agreement with published data from calorimetric measurements, 41.4 kJ/mol for propane[33] and 70 kJ/mol (at low coverages) for n-hexane.[34] Assuming that heats of adsorption for normal alkanes in MFI increase by 10 kJ/mol for each —CH_2—,[33] the agreement for n-octane is also reasonable.

An analysis of HC-trapping measurements with iso-pentane in BEA zeolites with varying Si/Al_2 ratios showed identical heats of adsorption, 51 ± 1 kJ/mol, on all of the samples. This result agrees with previous observations that interactions between alkanes and the acid sites are negligible at these low temperatures.[34] However, our measurements showed that the elution times and peak shapes varied with sample. As the equilibrium constants should depend only on zeolite structure, we examined how the effective zeolite fraction, a, and experimentally determined pore volumes would change the results.

In Figure 5, the measured peak elution times for the various BEA samples shown in Table 1 are plotted as a function of the pore volumes determined in TGA measurements of iso-pentane. There is a clear correlation between these variables, with the peak elution time increasing with pore volume. To determine how strongly elution time should vary with pore volume, we calculated the expected peak elution time as a function of a, taking into account that a is directly proportional to the pore volume. The solid line in Figure 5 is the result of this calculation, using the data for BEA38 as the starting point and varying only a, which is proportional to pore volume. The calculations explain the data well, especially given the uncertainty in the measured pore volumes. It is worth noting that aging affected the samples with lower Si/Al_2 ratios much more strongly. High-temperature steaming of zeolites is known to be particularly damaging to materials with lower Si/Al_2 ratios, as it will remove Al from the

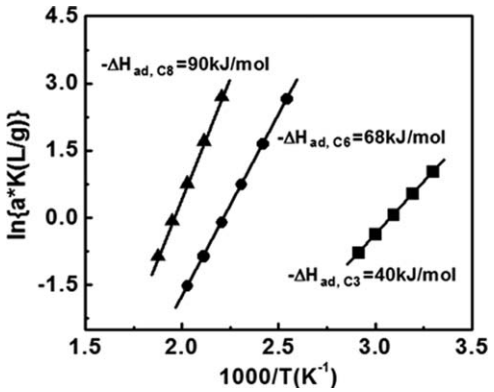

Figure 4. Heats of adsorption for alkanes on MFI280: (■) propane, (•) *n*-hexane, (▲) *n*-octane.

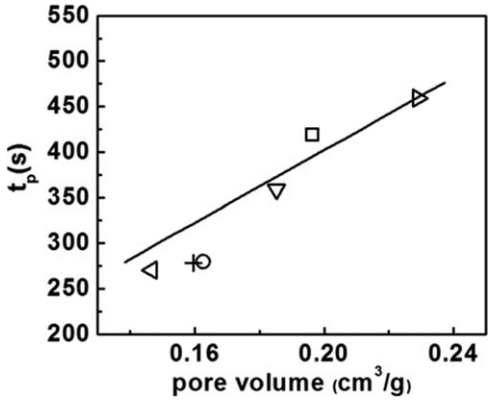

Figure 5. Correlations between iso-pentane peak elution times at 393 K and BEA zeolite pore volumes: (□) BEA24, (◁) BEA24 aged, (▷) BEA38, (▽) BEA38 aged, (○) BEA200, (+) BEA200 aged.

The solid line was calculated by varying effective zeolite fraction, which is proportional to pore volume.

framework and at least some of this nonframework material is likely to remain in and partially fill the pores.

Vehicle exhaust contains approximately 12% water and this can strongly affect the performance of hydrocarbon trapping. To determine how water influences this process, we carried out HC-trapping measurements with iso-pentane as a function of the background water pressure over BEA38 and BEA200 at 373 and 413 K. Results for BEA38 are shown in Figure 6a for background water concentrations of 0, 5.4, and 10.9%. At 373 K, the effect of increasing water concentration was dramatic and similar to the effect of changing $a \times K$ in Figure 3b in that there was both a decrease in the peak elution time and in the width of the peaks. With 10.9% water, the elution time was only 43% of its value under dry conditions. The percent change in the elution time was somewhat lower at 413 K, but still significant. The corresponding experiments on BEA200 are shown in Figure 6b. The changes on addition of water are much smaller; at 373 K, the elution time in 10.9% water was still 79% of its value under dry conditions.

The primary reason for changes observed in the presence of water vapor is due to changes in the available pore volumes for iso-pentane due to the presence of adsorbed water. Essentially, the apparent equilibrium constants are decreased for the same reasons as that found in Figure 5. On BEA38, there will be a significant uptake of water in the pores of the zeolite due to interaction with the Brönsted sites. It is well known that water tends to form clusters about these sites, so that uptakes can be significantly larger than one water molecule per site.[35,36] The uptake of water in the more siliceous zeolite, BEA200, will be less; however, there will still be adsorption, particularly at defect sites.[36]

With HC-trapping in the presence of steam, the temperature will affect both the hydrocarbon adsorption-equilibrium constant and the water coverage, so that the analysis used in Figure 4 for determining heats of adsorption for the hydrocarbon in the presence of water is not appropriate. However, it is noteworthy that the calculated equilibrium constants for iso-pentane in BEA200 were more strongly temperature-dependent than they were in BEA38, as shown in Table 2. The reason for this is that increasing the temperatures significantly decreased the loading of water in BEA38, increasing

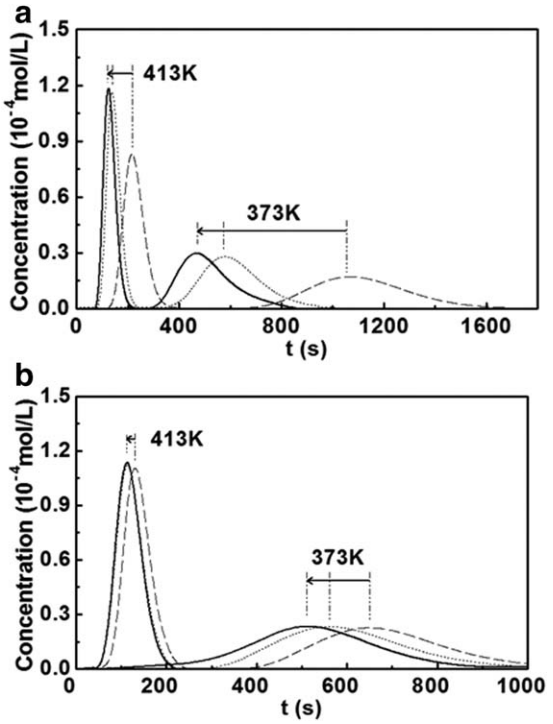

Figure 6. Iso-pentane adsorption on (a) BEA38 and (b) BEA200 in presence of water: dash line (---) 0% water, dotted line (···) 5.4% water, solid line (—) 10.9% water

the available pore volume for hydrocarbons, while the water loading was low at all temperatures for BEA200.

Discussion

Hydrocarbon trapping in automotive catalyst systems has a natural chromatographic signature associated with adsorption, desorption, and reaction of different HC species in zeolite materials in the ubiquitous presence of water vapor. This study shows that much of this chromatographic character can be emulated in a laboratory chromatographic adsorber that is simple in design and yet capable of generating fundamental data of direct utility in HCT design. Furthermore, the good agreement between the experimental data and a simple analytically solvable HC-adsorption model provides transparency (often lacking in vehicle studies) regarding the zeolite properties that affect HCT performance and the changes that occur on aging.

For alkanes, which adsorb primarily through van der Waals interactions with the zeolites, our studies show that equilibrium models describe the elution curves well and demonstrate that, for our conditions, kinetic limitations are negligible. The equilibrium data for pure compounds obtained from the chromatographic adsorption experiments

Table 2. The Calculated Heat of Adsorption of Iso-Pentane on BEA Zeolite in Presence of Water

Water Concentration (%)	$-\Delta H$ (kJ/mol)	
	BEA38	BEA200
0	51.4	50.6
5.4	45.5	50.4
10.9	42.9	50.1

agree well with conventional methods such as calorimetry; furthermore, there is a relatively simple and direct relationship between the elution time and both the equilibrium constant and the adsorption capacity of the trapping material. Most importantly, the chromatographic measurements allow the effects of coadsorbed water and zeolite aging to be determined quickly and easily. The experimental results, along with the model, can be used in a straightforward manner to make first-order projections of the HCT size required to (1) adsorb hydrocarbons without slip and (2) release the hydrocarbons at times and temperatures compatible with light-off of a TWC overlayer. Moreover, the chromatographic adsorption data can be input into more detailed reactor models that account for heat and mass transfer effects, as well as effects of water condensation and readsorption, to make more accurate calculations of the effects of trap size and location on overall HC conversion efficiency.

Even in the simple demonstration of chromatographic adsorption (and associated modeling) presented here, several observations emerge that provide useful HCT design guidance. Perhaps most significant is the importance of the effective zeolite fraction, a, which relates directly to the effective zeolite pore volume. Prior HCT design work at Ford has focused on maximizing zeolite washcoat loading for a fixed trap volume set by existing converter designs and packaging space. As shown clearly in Figure 5, however, the hydrocarbon elution times scale directly with pore volume, and vary by more than 35% for a range of BEA zeolite samples of different Si/Al_2 ratio and aging status. Thus, pore volume (and its retention after aging) is an important material property that must be weighed against other properties such as Si/Al_2 ratio in optimizing the zeolite for a particular application.

The simple chromatographic experiments conducted here also provide guidance in how to assess the effects of water vapor in gas mixtures, where the partial pressure of water exceeds that of the hydrocarbons by 2 to 3 orders of magnitude. Our results indicate that water competes with small alkanes for pore volume in the zeolite and suggest possible ways to minimize the effects of water on HC traps. Water molecules adsorb primarily on Brønsted sites, where they tend to form clusters with multiple molecules per site,[35] whereas alkanes show no preference for adsorption on Brønsted sites.[34] Prior to this work, there had been an assumption that Brønsted sites are required for effective trapping of olefins and ethanol, which are known to both adsorb and react at acid sites.[37,38] However, the competing effects of water adsorption, combined with the instability of the acid sites under hydrothermal aging conditions, suggest that at least part of the zeolite in a HCT should consist of high-silica, nonacidic materials.

Finally, this study clearly shows the challenge in storing weakly adsorbed hydrocarbons such as propane (see Figure 4) to temperatures where they can be reacted by the TWC overlayer. For van der Waals interactions, adsorption is enhanced in zeolites with smaller pores.[33] For example, the heat of adsorption for propane has been shown to increase from less than 30 kJ/mol in siliceous UTD-1 (a 14-membered-ring, one-dimensional-pore zeolite) to almost 50 kJ/mol in TON (a 10-membered-ring, one-dimensional-pore zeolite).[33] The effect this has on the equilibrium constants is dramatic. Obviously, the large-pore zeolites have the advantage of adsorbing aromatics and other larger molecules. Therefore, it may be advantageous to use a mixture of small- and large-pore zeolites in the trap, with the small-pore sieves there to capture the lighter hydrocarbons.

Conclusions

Catalyzed HCTs offer a potentially attractive method for improved cold-start technologies in three-way catalysts. This study has demonstrated the utility of a simple laboratory chromatographic adsorber for determining adsorption properties relevant to HCT design. Using simple alkanes, we have shown that zeolite adsorption capacities and adsorption equilibrium constants are key variables for controlling the uptake and elution of hydrocarbons. Water vapor affects adsorption by partial filling of the pores but the use of high-silica zeolites can reduce the effects. The equipment and instrumentation utilized here allow extension of the chromatographic adsorption approach to other hydrocarbons and organic species such as olefins and ethanol, thus opening the door to combined adsorption/reaction experiments under both isothermal and temperature-programmed column operation. Experiments of that type are in progress.

Acknowledgments

We acknowledge support from the Ford Motor Company University Research Program and from the Catalysis Center for Energy Innovation, an Energy Frontier Research Center funded by the U.S. Department of Energy, Office of Science, Office of Basic Energy Sciences under Award no. DE-SC0001004. Thanks are also due to Yisun Cheng and Manish Sharma for help with the experiments and the simulations.

Notation

C = alkane concentration in gas phase (mol/L)
C_0 = alkane concentration of inlet pulse (mol/L)
n = alkane concentration adsorbed on zeolite surface (mol/g)
t = elution time (s)
t_0 = injection time (s)
U = linear velocity in zeolite bed (m/s)
L = bed length (m)
A = column cross section area (m^2)
ε = bed porosity (m^3/m^3)
ρ = zeolite density (g/L)
K = equilibrium constant (L/g)
D = axial dispersion coefficient (m^2/s)
a = effective zeolite fraction (g/g)
Pe = Peclet number = UL/D

Literature Cited

1. Otto K, Montreuil CN, Todor O, McCabe RW, Gandhi HS. Adsorption of hydrocarbons and other exhaust components on silicalite. *I&EC Res*. 1991;30:2333–2340.
2. Li H-X, Donohue JM, Cormier WE, Chu YF. Application of zeolites as hydrocarbon traps in automotive emission controls. *Stud Surf Sci Catal*. 2005;158:1375–1382.
3. Liu X, Lampert JK, Arendarskiia DA, Farrauto RJ. FTIR spectroscopic studies of hydrocarbon trapping in Ag+-ZSM-5 for gasoline engines under cold-start conditions. *Appl Catal B*. 2001;35:125–136.
4. Czaplewski KF, Reitz TL, Kim YJ, Snurr RQ. One-dimensional zeolites as hydrocarbon traps. *Microporous Mesoporous Mater*. 2002; 56:55–64.
5. Burke NR, Trimm DL, Howe RF. The effect of silica:alumina ratio and hydrothermal ageing on the adsorption characteristics of BEA zeolites for cold start emission control. *Appl Catal B*. 2003;46:97–104.
6. Kanazawa T, Development of hydrocarbon adsorbents, oxygen storage materials for three-way catalysts and NOx storage-reduction catalyst. *Catal Today*. 2004;96:171–177.

7. Kaspar J, Fornasiero P, Hickey N. Automotive catalytic converters: current status and some perspectives. *Catal Today*. 2003;77:419–449.
8. Elangovan SP, Ogura M, Davis, ME, Okubo T. SSZ-33: a promising material for use as a hydrocarbon trap. *J Phys Chem B*. 2004;108: 13059–13061.
9. Elangovan SP, Ogura M, Zhang Y, Chino N, Okubo T. Silicoaluminaphosphate molecular sieves as a hydrocarbon trap. *Appl Catal B*. 2005;57:31–36.
10. Elangovan SP, Ogura M, Ernst S, Hartmann M, Tontisirin S, Davis, ME, Okubo T. A comparative study of zeolites SSZ-33 and MCM-68 for hydrocarbon trap applications. *Microporous Mesoporous Mater*. 2006;96:210–215.
11. Serrano DP, Calleja G, Botas JA, Gutierrez FJ. Characterization of adsorptive and hydrophobic properties of silicalite-1, ZSM-5, TS-1 and Beta zeolites by TPD techniques. *Sep Purif Technol*. 2007;54:1–9.
12. Iliyas A, Zahedi-Niaki MH, Eic M, Kaliaguine S. Control of hydrocarbon cold-start emissions: a search for potential adsorbents. *Microporous Mesoporous Mater*. 2007;102:171–177.
13. Sarsha R, Zahedi-Niaki MH, Huang Q, Eic M, Kaliaguine S. MTW zeolites for reducing cold-start emissions of automotive catalysts. *Appl Catal B*. 2009;87:37–45.
14. Park JH, Park SJ, Ahn HA, Nam I-S, Yeo GK, Kil JK, Youn YK. Promising zeolite-type hydrocarbon trap catalyst by a combinatorial approach. *Microporous Mesoporous Mater*. 2009;117:178–184.
15. Lopez JM, Navarro MV, Garcia T, Murillo R, Mastral AM, Varela-Gandia FJ, Lozano-Castello D, Bueno-Lopez A, Cazorla-Amoros D. Screening of different zeolites and silicoaluminophosphates for the retention of propene under cold start conditions. *Microporous Mesoporous Mater*. 2010;130:239–247.
16. Navarro MV, Puertolas B, Garcia T, Murillo R, Mastral AM, Varela-Gandia FJ, Lozano-Castello D, Cazorla-Amoros D, Bueno-Lopez A. Experimental and simulated propene isotherms on porous solids. *Appl Surf Sci*. 2010;256:5292–5297.
17. Moden B, Donohue JM, Cormier WE, Li HX. The uses and challenges of zeolites in automotive applications. *Top Catal*. 2010;53: 1367–1373.
18. Iliyas A, Zahedi-Niaki MH, Eic M. One-dimensional molecular sieves for hydrocarbon cold-start emission control: Influence of water and CO_2. *Appl Catal A*. 2010;382:213–219.
19. Hiramoto Y, Takaya M, Yamamoto S, Okada A. Development of a new HC-adsorption three-way catalyst system for partial-ZEV performance. *SAE Tech Paper*. 2003;01:1861.
20. Murakami K, Tominaga S, Hamada I, Nagayama T, Kijima Y, Katougi K, Nakagawa S. Development of a high performance catalyzed hydrocarbon trap using Ag-zeolite. *SAE Tech Paper*. 2004;01: 1275.
21. Mukai K, Kanesaka H, Akama H, Ikeda T. Adsorption and desorption characteristics of the adsorber to control the HC emission from a gasoline engine. *SAE Tech Paper*. 2004;01:2983.
22. Kidokoro T, Hoshi K, Hiraku K, Satoya K, Watanabe T, Fujiwara T, Suzuki H. Development of PZEV exhaust emission control system. *SAE Tech Paper*. 2003;01:0817.
23. Yamamoto S, Matsushita K, Etoh S, Takaya M. In-line hydrocarbon (HC) adsorber system for reducing cold-start emissions. *SAE Tech Paper*. 2000;01:0892.
24. Lupescu J, Chanko T, Richert J, DeVries J. Treatment of vehicle emissions from the combustion of E85 and gasoline with catalyzed hydrocarbon traps. *SAE Int J Fuels Lubr*. 2009;2:485–496; also SAE Tech Paper. 2009;01:1080.
25. Nunan J, Lupescu J, Denison G, Ball D, Moser D. HC traps for gasoline and ethanol applications. *SAE Tech Paper*. 2013;01:1297.
26. Ball D, Moser D. Cold start calibration of current PZEV vehicles and the impact of LEV-III emission regulations. *SAE Tech Paper*. 2012;01:1245.
27. LEV-III Emission Standards. California Air Resources Board, *Record Number*: N02823, 2012.
28. Carberry B, Grasi G, Guerin S, Jayat F, Konieczny R. Pre-turbocharger catalyst–fast catalyst light-off evaluation. *SAE Tech Paper*. 2005;01:2142.
29. Ruthven DM. Principles of Adsorption and Adsorption Processes, New York: Wiley, 1984:29–62.
30. Sarsani VSR. Solid acid catalysis in liquid, gas-expanded liquid and near-critical reaction media: investigations of isobutane/butene alkylation and aromatic acylation reactions, PhD Thesis, IIT Bombay, 2001:126.
31. Levenspiel O. *Chemical Reaction Engineering*, 3rd ed. New York: Wiley, 1999:293–320.
32. Shen DM, Rees LVC. Study of fast diffusion in zeolites using a higher harmonic frequency-response method. *J Chem Soc-Faraday Trans*. 1994;90:3011–3015.
33. Savitz S, Siperstein F, Gorte RJ, Myers AL. Calorimetric study of adsorption of alkanes in high-silica zeolites. *J Phys Chem B*. 1998; 102:6865–6872.
34. Savitz S, Myers AL, Gorte RJ, White D. Does the cal-ad method distinguish differences in the acid sites of H-MFI? *J Am Chem Soc*. 1998;120:5701–5703.
35. Lee CC, Gorte RJ, Farneth WE. Calorimetric study of alcohol and nitrile adsorption complexes in H-ZSM-5. *J Phys Chem B*. 1997; 101:3811–3817.
36. Olson DH, Haag WO, Borghard WS. Use of water as a probe of zeolitic properties: interaction of water with HZSM-5. *Microporous Mesoporous Mater*. 2000;35–6:435–446.
37. Kofke TJG, Gorte RJ. A temperature-programmed desorption study of olefin oligomerization in H-ZSM-5. *J Catal*. 1989;115:233–243.
38. Aronson MT, Gorte RJ, Farneth WE. The influence of oxonium ion and carbenium ion stabilities on the alcohol/H-ZSM-5 interaction. *J Catal*. 1986;98:434–443.

Manuscript received Oct. 9, 2013, and revision received Apr. 11, 2014.